

Colonic content assessment from MRI imaging using a semi-automatic approach

V. Ceballos¹ and E. Monclús¹ and P.-P. Vázquez¹ and A. Bendejú² and M. Mego² and X. Merino³ and F. Azpiroz² and I. Navazo¹

¹ViRVIG Group, UPC-BarcelonaTech, Barcelona, Spain

²Digestive System Research Unit, University Hospital Vall d'Hebron, Centro de Investigación Biomédica en Red de Enfermedades Hepáticas y Digestivas (Ciberehd); Universitat Autònoma de Barcelona, Barcelona, Spain

³Radiology Department, University Hospital Vall d'Hebron, Barcelona, Spain

Abstract

The analysis of the morphology and content of the gut is necessary in order to achieve a better understanding of its metabolic and functional activity. Magnetic resonance imaging (MRI) has become an important imaging technique since it is able to visualize soft tissues in an undisturbed bowel using no ionizing radiation.

In the last few years, MRI of gastrointestinal function has advanced substantially. However, few studies have focused on the colon, because the analysis of colonic content is time consuming and cumbersome.

This paper presents a semi-automatic segmentation tool for the quantitative assessment of the unprepared colon from MRI images. The techniques developed here have been crucial for a number of clinical experiments.

Categories and Subject Descriptors (according to ACM CCS): I.3.8 [Computer Graphics]: Applications— I.4.6 [Image Processing and Computer Vision]: Segmentation— J.3 [Life and Medical Science]: Health—

1. Introduction

Colonic content analysis is relevant for the diagnosis of functional intestinal disorders, such as constipation, diarrhea and irritable bowel syndrome; as well as to better understand the colon function under different dietary conditions [BMM*17]. In some functional gut disorders, featuring abdominal bloating and distension, the variation of intestinal gas content and its distribution has helped to understand the origin of the symptoms [BQA*13, BBA*15]. Moreover, the analysis of the effect of different diets in normal subjects in order to establish some information in normal conditions can help to identify abnormalities in relation to different symptoms. Through the analysis of Computed Tomography (CT) images of the patients, Azpiroz *et al.* obtained a better comprehension of the abdominal bloating and distension associated to different functional digestive diseases [APA*08, APA*09, MMPN*13]. Unfortunately, the X-ray radiation limits its application for this type of physiological diseases due to its low relative danger.

Magnetic Resonance Imaging (MRI) has become an important modality technique since it is able to visualize soft tissues without using ionizing radiation [CVC*95]. MRI acquisition techniques allow the modification of the signal emitted in order to acquire the different tissues presented in the body. The MRI sequences commonly used for the analysis of the colonic content are T2-weighted (T2) and T1-weighted Fat-Sat (T1-FS). However, those techniques, by themselves, do not allow for a proper classification

of the colonic content. In T2 images, the colon boundary is well-defined in the presence of fat around the colon, since it helps to define the limits of the colon morphology; but the intensity of the interior pixels does not identify the colonic content (for instance, black pixels could be gas or solid matter, see Fig 1). On the other hand, in T1-FS modality solid is well-defined but gas and fat are poorly contrasted, so the colon morphology can not be identified with high precision. As it can be observed in Fig 1 (see coloured circles), black pixels in T2 images could correspond to gas (orange circle) or stool (green circle) in T1-FS images. So, in order to carry out a quantitative assessment of the morphology and the colon content, both imaging sequences are required. Furthermore, in order to understand the normal behaviour of the gut under some specific conditions, it is necessary to acquire the abdomen without preparation, e.g., administration of drugs or contrast. So, in this kind of studies, it is necessary to use a medical imaging technique that allows the analysis of the colon in its *natural, normal* state.

This paper presents a semi-automatic segmentation tool for the quantitative assessment of the unprepared colon on MR images. Our approach uses T2-weighted HASTE (T2) and T1-weighted VIBE Fat-Sat (T1-FS) images for extracting all the information needed for the quantitative assessment. The use of both modalities allows the extraction of quantitative information on the colon morphology in the different segments (ascending, transverse, de-

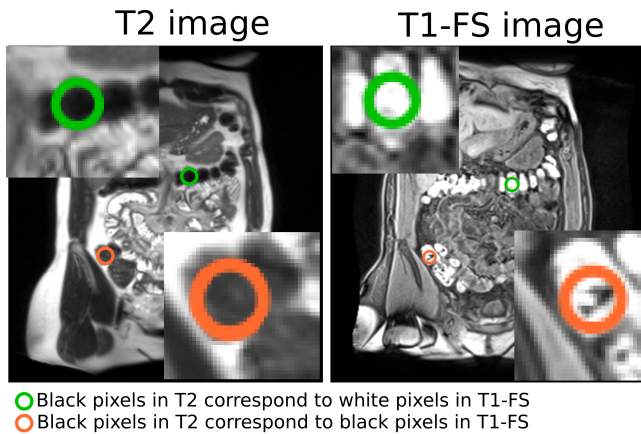


Figure 1: Differences between T1-FS and T2 MRI modalities for the same abdomen region. Black pixels in T2 (left) may correspond to gas (orange circle) or stool (green circle) in T1-FS images (right).

scending and pelvic) and the discrimination between the gas and non-gaseous (solid) content.

Specifically, we have developed an interactive colon segmentation tool from T2 images (Section 3.1 gives a detail description of it). Based on this colon segmentation, the contributions of our paper are:

- An automatic registration method that transfers the colon segmentation from T2 images to T1-FS images.
- An automatic classification method of the colon content from T1-FS images in order to obtain the amount of faecal content (non-gaseous).
- Different clinical experiments have been developed to evaluate each step of the overall process in an isolated way.

Throughout the system development, physicians, closely collaborated to establish the requirements of the functionalities, and the required levels of user intervention.

2. Previous work

There are a large number of previous research devoted to colon segmentation on CT since it is a fundamental preprocessing step in medical applications such as colon polyp detection, virtual colonoscopy or virtual colon unfolding. CT colon segmentation is mainly based on a combination of seed growing, morphological operators and thresholding. The algorithms usually require datasets obtained from prepared patients' colon in order to remove the colonic contents [NY08, BWKG01, SZBN08, LZ13]. On the other hand, the CT-based techniques used to segment the colon and to quantify its content [MMPN*13] are not applicable to MRI images because the information captured by MRI devices is not directly related to the colon content (in T2-MRI) or it is very complicated (even for radiologists) identify the border of the colon (in T1-MRI).

Moreover, MRI segmentation techniques used to identify other

anatomical organs (such as liver, brain, ...) are also not transferable to the segmentation of unprepared colon due to, among other effects: the colon motility, the quality of the images (low contrast between colon and its neighbor structures) and the variation of the intensity range inside the different parts of the colon due to the colon content.

In the last few years, MRI evaluation of gastrointestinal function has advanced substantially [ASM15]. Pritchard *et al.* [PMG*14] obtained a 3D reconstruction of the colon by 2D manual segmentation on T2-weighted images using the Analyze9TM software. On each coronal image slice, they manually outlined each colon segment (ascending, transverse and descending). From the 3D reconstruction they computed the volume of each colon segment. Volume information of the colon allowed them to carry out some experiments in order to infer the normal volume range of the regions of the colon in 75 healthy volunteers and 25 IBS-D (irritable bowel syndrome with diarrhea) patients. The authors acknowledged that the identification of the colon is a very time-consuming task, hence costly, and thus unpractical for its clinical application.

Sandberg *et al.* [SNP*15], developed a semi-automatic segmentation method for the quantification of the colon content from a manual segmentation over the T2-weighted images. From the segmentation of the colon on T2-weighted images, the software obtains, automatically, the segmentation of the colon on LAVA-Flex (T1-FS) images using a rigid registration process. After that, the segmentation of the faecal content within the colon is performed using a classification step. Their method has been used in different clinical experiments [PMB*18]. More recently, Mark *et al.* [MBG*19] used a slight modification of the same approach to investigate the effect of axycodone on colonic faecal volume. Their main limitation to be used in the daily clinical practice is the high amount of time devoted by the specialists.

Although it is out of scope of our proposal, another area where MRI has been started to be applied is in the analysis of colon motility. The use of cine-MRI has allowed to understand colon motility in a 2D acquisition plane of a specific colon segment in different conditions during a specific time interval [JSNS17, HMG*16].

3. Colonic Content Analysis

As introduced previously, the assessment of the colon content is carried out analyzing two different scans: T2 images allow the identification of the colon morphology and the use of T1-FS images helps us to establish the colon content.

The pipeline of the application is shown in Fig. 2. The patient is scanned twice to obtain T1-FS and T2-weighted images. Once the images are captured, the first task carried out by the physician is the interactive segmentation of the colon in T2 images (*colonSegT2*). Next, the registration between T2 and T1-FS is carried out using an automatic approach; the output of this process is the colon segmentation in T1-FS (*colonSegT1*). Finally, the non-gaseous and the gaseous colonic content are measured using both segmentations: *colonSegT2* and *colonSegT1*.

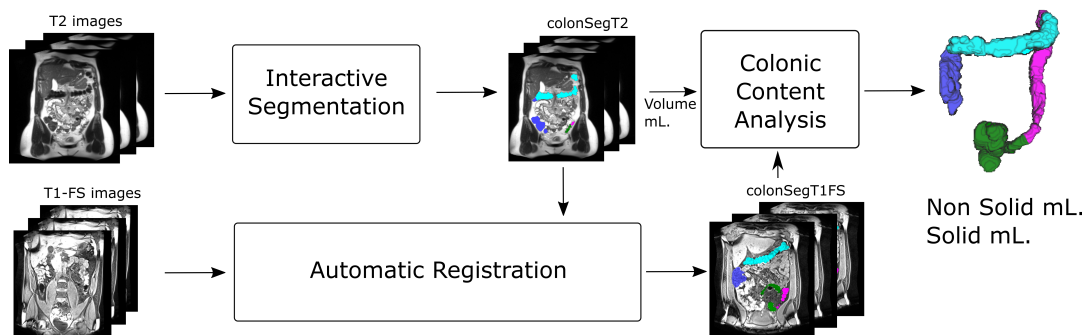


Figure 2: Workflow of the system: colon content is achieved using T2 to identify the morphology and T1-FS to establish its content.

3.1. Colon segmentation from T2 images

Our software provides a module for the segmentation of the colon morphology in the T2 images (Fig. 3 shows the workflow to segment the colon on T2 images). First, an anisotropic contrast enhancement filter (Perona’s Maliki diffusion) is applied to the images to enhance the colon boundary without losing details in the interior. Then, the user manually places some seed points on each image. The expansion of these seed depends on the gray-level mapping defined by the window-level setting of the images. More specifically the region growing algorithm is based on the combination of different sources of images to control the expansion of it: the original images after applying them a bilateral filter and also an edge-detector filter based on the zero-crossing of the Laplacian. The region-growing process may need some user intervention in regions where the colon contour is not well defined because of surrounding tissues having the same gray-level intensity. To solve this problem, we have implemented a set of interactive tools to facilitate the colon segmentation in these regions. We carefully designed the specialist interaction to reduce the user effort (i.e., mouse displacements) and the time consumed. The toolkit includes techniques used in photo/image edition such as pen, eraser, and shape tools, and a restricted expansion of the region-growing algorithm. For instance, if the user clicks in a pixel that belongs to a current segmentation, depending on the button clicked, the region-growing algorithm expansion is fixed to a pixel-neighborhood size. This tool gives to the specialist a finer control of how the segmented regions expand (Fig. 4 shows a capture of the application GUI).

Once the colon segmentation is completed, the different colon regions (ascending, transverse, descending, and pelvic) must be identified. This task is eased by using a 3D view of the colon, and providing a tool that lets the user simply place a line which represents the intersection of a plane with the 3D view. Each plane separates two different regions. Once this is done, our software automatically re-classifies the colon segmentation according to the introduced information.

Section 4.2 describes the experiments performed in order to determine the accuracy of the obtained segmentation in terms of the total colon volume computed and also its applicability to clinical practice with respect to the level of reproducibility achieved.

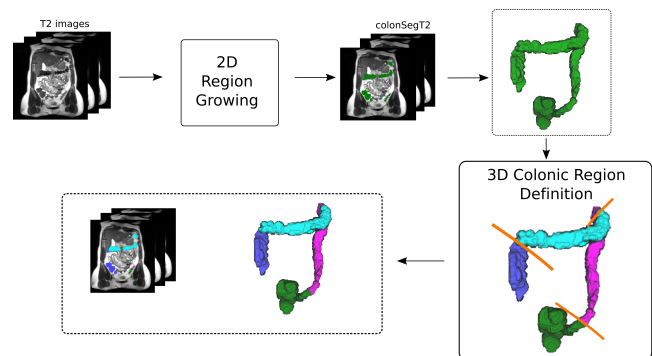


Figure 3: Colon workflow segmentation from T2 images. First, the colon is identified on each of the T2 images. Then, the user defines the different colon regions by using the 3D representation.

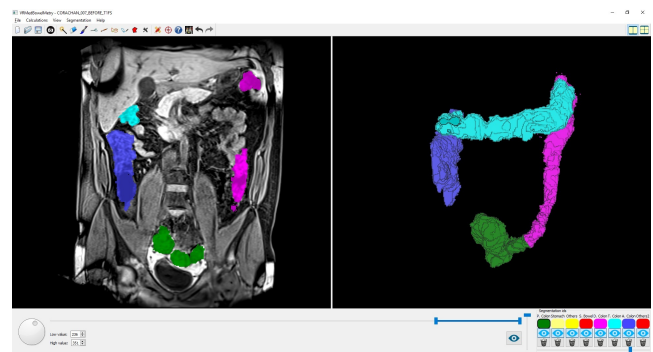


Figure 4: Snapshot of the developed application. The different techniques tailored to colon segmentation are depicted in the upper toolbar. When a technique is selected, the bottom toolbar shows the configuration option of the selected technique.

3.2. Registration process between T2 and T1-FS images

As previously indicated, T2 images do not distinguish clearly all the materials/tissues inside the colon (see Fig. 1). By contrast, T1-FS images allow the identification of the solid material properly (bright areas correspond to solid/water material) but colon bound-

ary cannot be identified with high precision since gas and fat are poorly contrasted. So, the calculation of the non-solid content can be inferred by subtracting the amount of solid to the total colon volume calculated from T2 images.

The manual identification of the solid content in T1-FS images using the same application tailored to colon segmentation on T2 images costs from 1 to 2.5 hours of intensive work for an experienced user to compute the segmentation of the solid material inside the colon. In order to make our approach useful for clinical practice, the user-interaction time needs to be extremely reduced.

We tackled the problem by using the previously segmented T2 images to register them to T1-FS images. Note that, although the capture of T1-FS modality images is consecutive to the capture of T2 images, the position of the colon may have changed from one acquisition to the other due to different reasons: first of all, the scans were obtained during an apnea, so depending on the level of the apnea, the position of the diaphragm and thereby the colon position may vary between the two scans. Also, the colon can change its shape and position very quickly and the acquisition time of T2 images is not instantaneous (each image sequence may take up to 40 seconds). Clearly, due to the nature of these movements, a rigid transformation approach is prone to errors.

After a thorough study of all the different registration strategies the *ANTs* package [ATS*11] provided, we found empirically that the best results were obtained using a deformable transformation (an elastic diffeomorphic transformation) with cross correlation as the similarity measure. The chosen method and the tuning of the different parameters were settled on empirically with the collaboration of the medical experts: we prepared a collection of different T1-FS sequences images registered using different appropriate methods for the characteristics of the images and let them to evaluate the results (in total we test 20 different registration strategies). The evaluation was performed by visual analysis of the registration result.

Once the deformation field from T2 to T1-FS images has been calculated, it is applied to the colon segmentation on T2 images (Fig. 5 presents the pipeline of the registration process). This way, the original T1-FS images remain undeformed and the colon segmentation computed on T2 images is deformed according to the deformation field. In this way, if the registration process introduced any segmentation error, medical experts had the possibility to fix them by analyzing the registered segmentation over the original undeformed T1-FS images. This task is performed interactively by using the same photo/image edition techniques developed for the colon segmentation on T2 images. Medical doctors considered that this technique was an easy and quick process, since it takes only 10 minutes to complete the T1-FS segmentation.

3.3. Colon content computation

As staged in previous sections, in T1-FS images, bright pixel intensities represent solid/water content. Once Step 2 of our proposal workflow has been executed (see Section 3.2), the colon has been identified on T1-FS images we proceed to automatically determine the colonic content. This process consists of classifying the pixel

intensities according to the percentage of solid content they represent. We established three categories:

Non-solid Pixel intensities which belong to this category contain 0% solid.

Uncertain-Solid Pixel intensities which belong to this category contain a percentage of solid which will be defined computationally.

Solid Pixel intensities which belong to this category are considered as 100% solid content.

The *Uncertain-Solid* category represents the range of pixel intensities which is not feasible to be classified by the human eye in the captured images. In other words, this category intends to capture the uncertainty aspect in medical image data.

The classification of pixel intensities within the colon is based on the k-means clustering algorithm [JM13]. We use several executions of this algorithm varying the number of clusters in order to empirically determine the bounds of the three categories defined above.

First, the pixel intensities are classified, using k-means, into three separate clusters. If we consider the two upper classes as solid material we obtain a good correlation with the bright pixel intensities of the images. So, we decided to use this value as the lower-bound of the *Solid* category. This value also corresponds to the upper-bound of the *Uncertain-Solid* category.

In order to determine the lower-bound of the *Uncertain-Solid* category, we do it empirically as well: as we increased the number of clusters into which pixels are classified using k-means, we observed that the first class (the lower class) was stabilized (convergence occurs at around 20 clusters). At this point, we consider the upper-bound of the *Non-solid* category as the limit of this first cluster. This value also corresponds to the lower-bound of the *Uncertain-Solid* category.

Once the range of pixel intensities belonging to the *Uncertain-Solid* category has been established, the amount of solid that corresponds to each pixel intensity has to be determined. In other words, the variation of solid content has to be defined over the range of pixel intensities that belong to this category. We have experimented three different mathematical models (solid, linear and data-captured) for computing the percentage of solid each pixel intensity represents. Being $[I_{min}, I_{max}]$ the range of intensity values of this category and vol the volume (in cubic milliliters) that a voxel represents; for any intensity value $I_x \in [I_{min}, I_{max}]$, the solid volume, vol_{I_x} , represented by this value can be computed as follows:

Solid $vol_{I_x} = 0$. This formulation assumes no uncertainty presented in the data. This formulation could be considered equal to the proposal of Sandberg et al. [SNP*15].

Linear $vol_{I_x} = vol * (I_x - I_{min}) / (I_{max} - I_{min})$

Data-captured (DC) using a piecewise linear function defined by the upper-bound values of the lower class of the clusterings from 3 clusters to 20 (Fig. 6 shows the description of this data-captured function). Let (I_{x_i}, y_i) represent the data-captured values: I_{x_i} is an intensity value and y_i maps the cluster were I_{x_i} is inside to the percentage of solid this cluster is supposed to represent. We assign to cluster 3 a 100% of solid volume and cluster

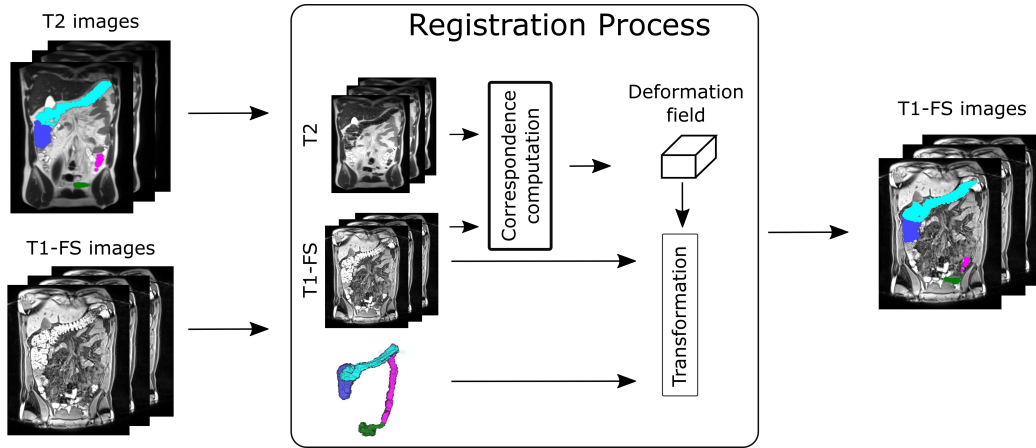


Figure 5: Registration process between T2 and T1-FS images. First, the deformation field from T2 to T1-FS images is computed. Then, it is applied to the colon segmentation from T2 image. The result is the colon segmentation in the original T1-FS images.

20 maps to 0% solid volume. The rest of clusters maps linearly proportional between these two values. Then:

$$vol_{I_x} = vol * \left(\frac{(I_x - I_{x_i}) * y_{i+1}}{I_{x_{i+1}} - I_{x_i}} + \frac{(I_{x_{i+1}} - I_x) * y_i}{I_{x_{i+1}} - I_{x_i}} \right) \text{ being } I_{x_i} < I_x < I_{x_{i+1}}$$

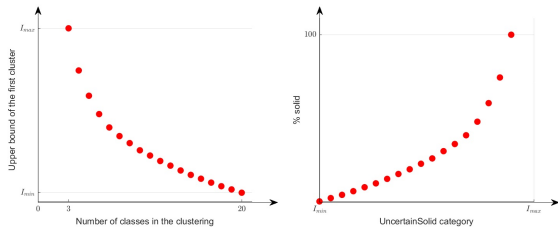


Figure 6: Approximation of the solid volume computation by the Data-Captured function. Using the different upper-bound values of the lower class resulting from the execution of the k-means algorithm using from 3 to 20 classes, the percentage of solid is approximated.

After testing the different mathematical models on the validation experiments, we conclude that the best results were obtained by using the *Data-captured* model (Section 4.4 gives a detailed explanation of the performed experiments).

Summarizing, the process to calculate the colon content from the segmentation of the T1-FS and T2 images consists of the following steps (Fig 7 shows the overall process):

1. Determine the lower-bound of the *Solid* category. This process involves applying a *k-means* clustering algorithm to the colon segmentation on T1-FS images using 3 classes.
2. Determine the upper-bound of the *Non-solid* category. This process involves applying a *k-means* clustering algorithm to the colon segmentation on T1-FS images using 20 classes.
3. Determine the specific values of the DC function. This process involves applying a *k-means* clustering algorithm to the colon segmentation on T1-FS images using from 3 to 20 classes.
4. Compute the solid volume of the colon. This process consists

of a traversal of the colon segmentation on the T1-FS images, adding the volume contribution of each pixel/voxel to the total volume.

5. Compute the gas volume of the colon. From the solid volume of the colon calculated in the previous step, the gas volume of the colon is equal to the total volume of the colon on T2 images minus the solid volume on T1-FS images.

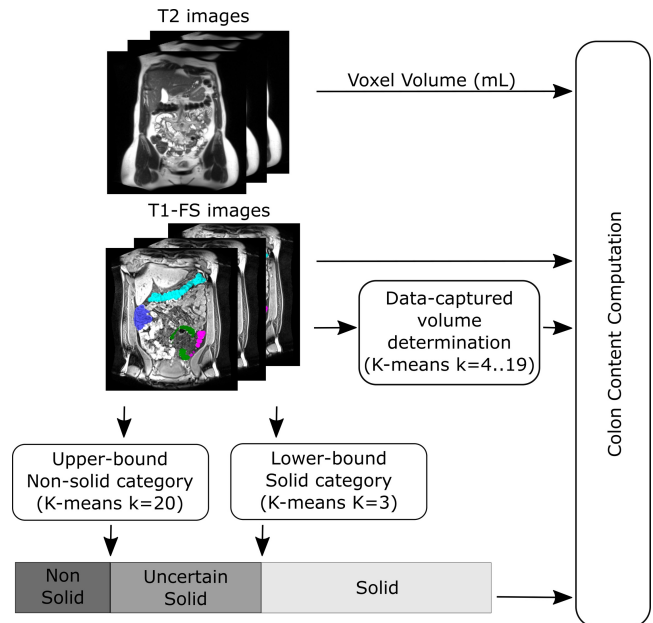


Figure 7: Colon content computation. This figure shows the pipeline for the colon content computation on T1-FS images.

The process explained above could be applied to the overall colon segmentation, however we have found that better results are obtained if it is apply to each segment of the colon separately. The clinical reason is that the colon contains more water inside the as-

ascending region, so the stool is blended with water. As the material travels around the colon, the water is absorbed by the intestine, so the stool becomes drier. This behaviour of the material is well reflected in the lower-bound of the *Solid* category computed with our process which decreases as we move along the colon (Note that, bright pixel intensities correspond to solid/water material). Fig 8 shows the variation of the lower-bound value for the *Solid* category over the ascending and the pelvic colonic regions for different datasets.

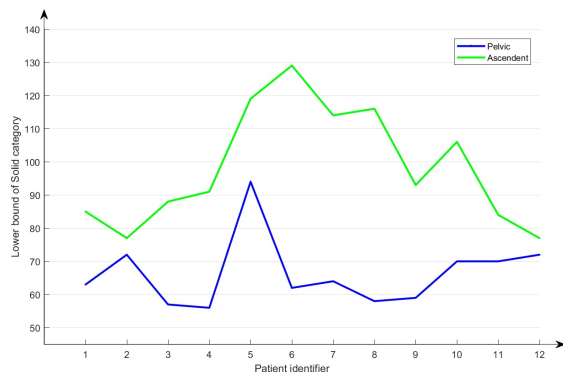


Figure 8: Solid lower-bound value variation in the ascending and the pelvic colonic regions. This chart shows how the lower-bound value for the Solid category varies over the ascending and the pelvic colonic regions. Horizontal axis represents the patient identifier and the vertical axis represents the intensity value of the lower-bound of the Solid category. As shown, the lower-bound value decreases along the colon traversal. This information is in accordance with the physiological meaning of intensity pixels along the colon. The content of water in the stool reduces in the course of the colon.

Section 4.4 gives a detailed explanation of the experiments carried out in order to determine the accuracy achieved.

4. Validation and Results

In this section, we explain the different experiments carried out to evaluate each step of the overall process in an isolated way:

- To calculate the inter-observer variability in the colonic volume measurement, 20 MRI chosen randomly were measured independently by two investigators.
- The validation of the colon volume using T2 images was performed by computing the colon volume before and after gas introduction, and comparing the difference to the real inflated gas volume.
- The validation of the amount of solid inside the lumen (using T1-FS images) consisted in computing it before and after a defecation, and comparing the difference to the real measured volume defecated.
- For the global validation of the all computed measurements (colon volume in T2 images and solid colon volume in T1-FS images), data provided from different experiments using abdominal computed tomography (CT) were used (a complete descrip-

tion can be found in [BBB*16]). These analyses allowed to establish colonic content and its distribution inside the lumen under different conditions and comparing it with respect the results of our proposal using MRI images.

The variables measured (volumes) are reported in mL as mean±standard deviation with range in brackets. The Kolmogorov-Smirnov test was used to check the normality of data distribution. All computed measurements were compared between the two observations by Student's *t*-test for paired and unpaired data. The differences between the computed measurements and the real ones were analyzed by Pearson correlation.

4.1. Patients and Images

Eighteen healthy subjects (11 women, 7 men) with a mean age of 35 years (24-55) participated in the study. The participants were instructed to complete a clinical questionnaire to confirm the absence of gastrointestinal symptoms; all reported normal bowel habits (7.0 ± 0.1 bowel movements per week) and stool form (3.9 ± 0.2 score on the Bristol scale) [LH97]. Subjects gave their written informed consent to participate in the study. The study protocol was previously approved by the Institutional Review Board of the University Hospital Vall d'Hebron.

Ten participants were scanned before and immediately after the rectal infusion of a known quantity of air (range 50-170 mL) using a rectal balloon catheter.

In fifteen participants a scan was performed before and after a spontaneous defecation. Participants were instructed to defecate in a disposable pan to measure the weight of stool using a digital weighing scale. Then, the stool volume was measured by immersing it in water within a graded beaker and recording the water level change.

In all the experiments, each time a subject was scanned, two coronal image series of the abdomen were obtained: one T2-weighted HASTE sequence during two apneas of approximately 20 seconds each. After that, a T1-weighted VIBE Fat-Sat sequence in one apnea of 12 seconds was acquired. No drugs or contrast were used in the capture.

Abdominal MRI scans were acquired using a 1.5 Tesla MRI System (Aera; Siemens Healthcare, Erlangen, Germany) with 2 six-channel phased-array abdominal coils to cover the whole abdomen. In all the experiments, each subject was scanned in breath holding using a T2-weighted HASTE sequence in the coronal plane (TR = 1400 ms, TE = 90 m, slice thickness 3.5-mm, flip angle = 180° , in-plane resolution 1.718 x 1.718 mm) and T1-weighted VIBE Fat-Sat sequence in the coronal plane (TR = 3.71 ms, TE = 1.66 ms, slice thickness 1.5 mm, flip angle = 10° , in-plane resolution 1.5 x 1.5 mm). T2 scans produced 50 contiguous slices with a resolution of 256 x 256 pixels. T1-FS scans produced 120 contiguous slices with a resolution of 270 x 320 pixels.

All images were codified and analyzed blinded to the source, acquisition, and any preceding intervention by two trained physicians in MRI images under the supervision of an expert radiologist.

4.2. Validation of the colon segmentation from T2 images

The reproducibility of the measurements was analyzed using Bland Altman plots [AB83] (see Fig. 9). No significant differences between the two observations were detected for any of the segments (p -value =0.989 for the total colon volume using a significance level of 0.05).

The measurements yield similar results for the total colonic volume between two investigators (701 ± 40 mL and 702 ± 37 mL, $p=0.515$) and for every colonic segment (188 ± 11 mL and 199 ± 1 mL ascending colon, 199 ± 11 mL and 199 ± 11 mL transverse colon, 157 ± 12 and 157 ± 10 descending colon, 157 ± 18 and 147 ± 16 pelvic colon). Table 1 shows the total and regional colon volumen for the two investigators and the p -value of the t-Student test. The results of the regional volumes of the colon are similar to those reported by Sandbergg et al. [SNP*15].

Region	Obs. A	Obs. B
Ascending	188 ± 11 (102-266)	199 ± 13 (108-306)
p -value	0.515	
ICC	0.942	
Traverse	199 ± 11 (67-308)	199 ± 11 (91-308)
p -value	0.993	
ICC	0.942	
Descending	157 ± 12 (49-242)	157 ± 10 (68-245)
p -value	0.995	
ICC	0.941	
Pelvic	157 ± 18 (70-407)	147 ± 16 (60-335)
p -value	0.67	
ICC	0.953	
Total	701 ± 40 (374-1107)	702 ± 37 (366-1019)
p -value	0.989	
ICC	0.973	

Table 1: Total and regional colon volumes obtained for the two investigators (Obs.A|B). For each colonic region: the colonic volume information is shown followed by the p -value of the t-Student test and the ICC coefficient.

In order to analyze the accuracy of the colon segmentation from T2 images we carried out an experiment where the difference between the colonic volume in T2 before and after rectal gas infusion was compared with the real gas introduced by the catheter. No statistics differences were found in the increase in colonic volume after rectal gas infusion and the real gas infused (117 ± 12 mL vs 116 ± 12 mL, Pearson's $\rho = 0.877$ and $p=0.01$). Table 2 shows the total colonic volume before and after gas infused with the measurements and the real gas infused. Fig. 10 shows a good correlation between computed values and the real ones. Note that a mean error of 10 mL is clinically insignificant.

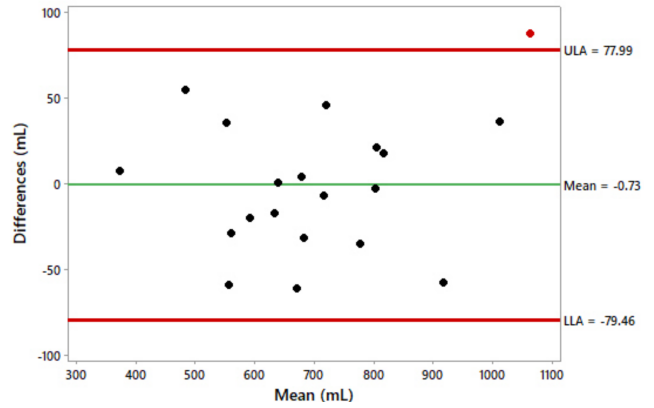


Figure 9: Bland Altman plot of the colonic volume measured on T2 images. Independent measurements of colonic volume by two observers yielded similar results for all the colon segments.

Total Colon Volume		Computed Gas	True Gas	Error
Before	After	Infused	Infused	
789	943	154	170	16
1150	1252	101	140	39
727	763	36	50	14
736	852	116	100	-16
838	968	130	150	20
629	770	141	160	19
749	908	159	140	19
Mean		120	130	10
Error St		15	8	15

Table 2: Total colon volume before and after infusion of gas. The mean and the standard error are also calculated for the variables analysed.

Furthermore, we wanted to measure the time used by the physicians to segment T2 images. For this purpose, we measured the spent time by the physician to complete this task in two different datasets. The colon segmentation takes 25 minutes to complete for an experimented physician (in both cases), which is considered by the physicians reasonable to be used in the daily practice.

4.3. Validation of the registration process

Validation experiments were also carried out to establish the accuracy of the automatic registration process. As mentioned before, once the automatic identification of the colon content has been calculated, medical experts have the possibility to correct all the bright areas of the registered segmentation which were wrongly identified. In order to establish the accuracy of the automatic process, we ask medical experts to add and/or erase all the bright regions which were misclassified by the automatic registration process. Medical experts had to accurately correct all the T1-FS abdominal scans explained in *Patients and Images* section (46 datasets). They con-

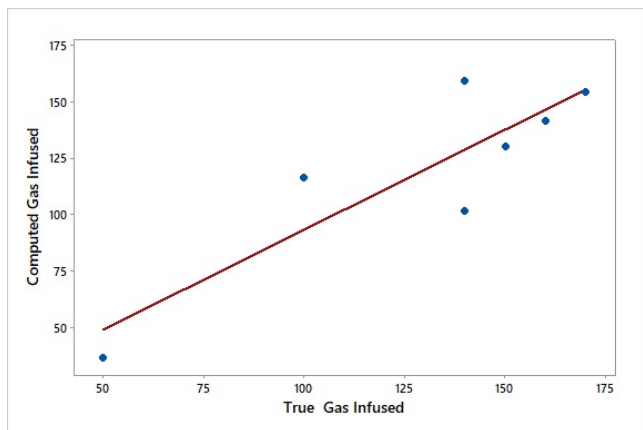


Figure 10: Correlation between the differences in colon volume before and after gas infused and the true gas infused. A significant linear association was found ($R^2 = 76.8\%$).

sidered it easy and quick to assess. On average, it takes only 10 min (range 8-13) to complete.

Comparing our approach with respect to the work of Sandberg *et al.* [SNP*15], the main difference relates to the type of registration used. Sandberg *et al.* uses a rigid transformation approach with mutual information as the similarity measure (they used the *elastix* registration package [KSM*10]). They mentioned that a rigid transformation only works well if both acquisitions were captured at the same breath hold position due to the level of the breath hold affects the position of the diaphragm and thereby the position of the transverse colon relative to the ascending and descending colon. Radiologists, we work with, consider this restriction not acceptable for the daily clinical practice. Moreover, in [MBG*19] where Sandberg *et al.* approach is used, they explained the same drawback we have already mentioned, so they decided to manually segment T1-FS images increasing, therefore, the devoted time by physicians.

In summary, the solid volume that physicians needed to add to the segmentation of the colon was on average 37.89 ± 24.19 mL (3.37-128.19). This amount was the solid volume within the colon which was missed by the registration algorithm. Moreover, 28.17 ± 20.38 mL (on average, with a range value 2.02-109.6) were misidentified as solid interior to the colon. After medical experts corrected all the T1-FS scans, we asked them to evaluate qualitative the feasibility of the application. The results we obtained were scored by physicians with 7 over 10.

4.4. Validation of the colon content computation

The validation of the computation of solid inside the lumen consisted in determining the accuracy achieved when computing the faecal volume, by comparing it to the real measured volume (as explained in Section 4.1, image sequences before and after defecation, were compared).

Table 3 shows the complete statistical analysis performed. Total colon volume is calculated from T2-weighted images. The calculated faecal volume (Defecated column) is calculated as the dif-

ference between the faecal amount in the before and after sequence images (T1-FS modality). The real defecated volume was measured as: mean 136 ± 20 , value range of (10-270) and with a MSE of 20.1.

Analysing the difference between the two acquisitions (*before - after*), the computed solid volume using DC formulation was 131 ± 102 mL, which agree with the real solid volume defecated (136 ± 20 mL, with a range values of (10-270) and an standard error $SE = 20.1$. Pearson's $\rho=0.612$ and $p=0.0015$).

Before		After		Defecated
Total	Faecal	Total	Faecal	
843 ± 150 (509-1106)	599 ± 111 (372-808)	685 ± 157 (352-951)	481 ± 117 (240-667)	118 ± 94 (14-372)
	684 ± 150 (73-888)		557 ± 157 (288-742)	126 ± 100 (0-101)
	730 ± 150 (413-935)		481 ± 117 (302-807)	131 ± 102 (0-423)

Table 3: Total and faecal colon volumes before and after an spontaneous defecation are reported. Faecal measurement was computed using the different formulations explained in section 3.3. Next rows show the computed results of Solid, Linear and Data Captured methods respectively.

4.5. CT results against MRI results

In previous works using CT images, information about colonic gas and colonic volume in a large cohort of healthy subjects were collected [BBB*16]. The colonic gas was 90 ± 102 mL, and the colonic solid volume in fast situation was 702 ± 184 mL which represent $90 \pm 9.26\%$ of the total volume (the application used for the computation of gas was explained in [MMPN*13]). This percentage was similar even in fed situation, and it has been taken as a clinical standard reference.

Table 4 shows the total colonic volume and its content obtained in our experiments with MRI datasets using the three methods for estimating the uncertain-solid presented in Section 3.3. The table also shows the results obtained by the specialists using a manual segmentation of T1-FS images for the same datasets. Additionally, the clinical standard values for CT data are shown. Medical experts analyzed the numerical results concluding that the Data Captured method is the most adequate. They argued that the manual segmentation was very difficult and could have some inaccuracies, so their preferred to take as reference the CT standard values.

This percentage was similar even in fed situation. The total colonic volume and its content calculated under the different ways are compared in table 4. We analyzed, together with the medical experts, the numerical results of the different ways of computing the faecal content using MRI images and also the numerical distribution of all the conditions with respect the computation using CT images. The result closest to the CT result was the *Data Captured* (DC) as shown in Table 4.

Solid Percentage				
Manual	Solid	Linear	DC	CT
74±13.04 (334-886)	67±6.4 (180-462)	81±7.67 (73-330)	87±7.56 (19-267)	84±77 (13-365)
Solid Volume				
626±147 (334-886)	561±104 (330-753)	684±129 (395-888)	730±139 (413-935)	702±184 (431-1166)
Gas Volume				
227±136 (60-554)	282±85 (180-462)	160±79 (73-330)	113±72 (19-267)	90±102 (15-491)
Colon Volume				
MRI				
843±150 (509-1106)			790±220 (457-1263)	

Table 4: Total colon volume is calculated from T2 images sequences. Total solid volume, solid percentage and gas volume are reported from the different formulations proposed.

5. Discussion

In summary, this paper presents a novel semi-automatic segmentation tool for quantitative assessment of the unprepared colon from MRI images. Our approach uses the T2-weighted HASTE (T2) and T1-weighted VIVE Fat-Sat (T1-FS) images for extracting all the information needed for the quantitative assessment.

Agreement between observers was really good as shown in Section 4. No significant differences between the two observations were detected for any of the segments (p -value = 0.989 for the total colon volume using a significance level of 0.05). Moreover, the segmented volumes were within expected range reported in previous studies. The accuracy of the identification of the colon volume was very good when comparing it with respect to the computed total volume in T2 sequences as reported in Section 4.

With respect the measured time spent by the physician to obtain the colon segmentation in T2 images, they argue that if the participant is very thin the lack of fat surrounding the colon makes this task more tiresome (in this case the overall time consumed can raise until 40 minutes).

Regarding the computation of the faecal content from T1-FS images several findings have to be taken into account in order to understand the results. According to Bendezú *et al.* [BBB*16], the expected solid volume is 85% with respect to the total colon volume. Note that colonic content and distribution were measured in CT scans using an original analysis program tailored specifically for this purpose [MMPN*13]. In order to obtain a good baseline of the solid content that a human-eye is able to classify, we asked medical doctors to manually segment a set of 32 T1-FS MRI scans (as exposed in 3.2, this task was performed by using the same application devoted to the colon segmentation on T2 images). The comparison between the obtained results and the expected amount of solid content inside the colon based on the analysis of CT im-

ages revealed the uncertainty presented in MRI images. Medical doctors were able to identify $73.47 \pm 16.2\%$ of solid volume inside the colon with respect to the total colon volume.

Furthermore, comparing our approach with the one presented in [SNP*15], the results they obtained are equivalent the ones we obtained if we consider that the *Uncertain-Solid* category represents 0% of the solid (and thus should be merged with the *Non-Solid* category). The approach of Sandberg *et al.* obtains an average faecal content ranging from 71% to 76% of the total colon volume for the different regions of the colon. Their results are in accordance with the results we obtained if a manual segmentation of T1-FS images is used. In fact, they compare their automatic classification with respect to a manual segmentation on T1-FS images; concluding the good correlation between both results. If we proceed in the same way, our results are very satisfactory in terms of the correspondence between the *Solid* category and the manual segmentation: $86.14 \pm 6.5\%$ of the volume of the manual segmentation belongs to the *Solid* category.

Moreover, in other experiments out of the context of this paper, we tested our proposal in different capturing devices concluding that all the empirical or heuristically decisions taken were working well without the need of being redefined again. Also, the system has been validated to be feasible for pathological cases in current experiments carried on by the specialists.

6. Conclusion

The semi-automatic segmentation tool for quantitative assessment of the unprepared colon from MRI images presented in this paper is currently being used by clinicians in experimental studies using abdominal MRI imaging. The resulting software greatly facilitates the analysis of images by reducing the time the users need to devote to achieve a segmentation and also achieves a better accuracy that the commercial packages present in the radiologic workstations. In particular, the application developed for colon segmentation using T2 modality was used in [BMM*17] for the manual segmentation of the colon in T2 images and the manual identification of the faecal content in T1-FS images. Thanks to it, several findings have been obtained with respect to the effects of meals, defecation, a diet on colonic content.

From the beginning of the software development, medical doctors participated in it by testing the different tools which were being developed. They provided practical input that helped decide the final work-flow of the application, as well as the interaction tools to use in order to achieve the best user-friendly GUI.

The total amount of time spent by a medical doctor in the assessment of the colonic content is reduced to 40 minutes in total (noting that 15 minutes are completely automatic so the physician can dedicate to other tasks).

The main limitation of our approach is the time devoted by the specialist to obtain the colon segmentation in T2 images and T1-FS images. Currently, the complete automatization of the overall workflow is being developed. We have done great advances in the automatization of the colon segmentation on T2 images (first results have been published in [OMB*18]). This improvement will

highly benefit the current application, as the entire process could then be executed requiring little input of physicians (just 5 minutes of user interaction). Although, the registration of T2 images to T1-FS is almost completely automatic, some user intervention is needed in order to obtain the most accurate segmentation on T1-FS images. We have started to explore other different registration techniques that takes advantage of all the restrictions in the deformation the colon do not allow. We have to take into account, as exposed in Section 5, that in most cases the differences between the images is only due to a difference between the apnea situation when the images were captured.

7. Acknowledgments

The authors want to thank all the participants involved in the experiments. This work has been partially supported by FEDER funds and the Spanish Ministry of Science, Innovation and University under the grants TIN2017-88512-C2-1-R, and SAF 2016-76648-R.

References

- [AB83] ALTMAN D. G., BLAND J. M.: Measurement in Medicine: The Analysis of Method Comparison Studies. *The Statistician* 32, 3 (Sept. 1983), 307–317. 7
- [APA*08] ACCARINO A., PEREZ F., AZPIROZ F., QUIROGA S., MALAGELADA J.: Intestinal gas and bloating: Effect of prokinetic stimulation. *Gastroenterology* 103 (2008), 2036–2042. 1
- [APA*09] ACCARINO A., PEREZ F., AZPIROZ F., QUIROGA S., MALAGELADA J.: Abdominal distention results from caudo-ventral redistribution of contents. *Gastroenterology* 136 (2009), 1544–1551. 1
- [ASM15] ALYAMI J., SPILLER R. C., MARCIANI L.: Magnetic resonance imaging to evaluate gastrointestinal function. *Neurogastroenterology & Motility* 27, 12 (2015), 1687–1692. 2
- [ATS*11] AVANTS B. B., TUSTISON N. J., SONG G., COOK P. A., KLEIN A., GEE J. C.: A reproducible evaluation of ANTs similarity metric performance in brain image registration. *NeuroImage* 54, 3 (2011), 2033–2044. 4
- [BBA*15] BARBA E., BURRI E., ACCARINO A., CISTERNA D., QUIROGA S., MONCLÚS E., NAVAZO I., MALAGELADA J., AZPIROZ F.: Abdominothoracic mechanisms of functional abdominal distension and correction by biofeedback. *Gastroenterology* 148, 4 (2015), 732–739. 1
- [BBB*16] BENDEZÚ A., BARBA E., BURRI E., CISTERNAS D., ACCARINO A., QUIROGA S., MONCLÚS E., NAVAZO I., MALAGELADA J. R., AZPIROZ F.: Colonic content in health and its relation to functional gut symptoms. *Neurogastroenterology and Motility* 28, 6 (2016), 6, 8, 9
- [BMM*17] BENDEZÚ A., MEGO M., MONCLÚS E., MERINO X., ACCARINO A., MALAGELADA J. R., NAVAZO I., AZPIROZ F.: Colonic content: effect of diet, meals, and defecation. *Neurogastroenterology and Motility* 29, 2 (2017), 12930–1–12930–8. 1, 9
- [BQA*13] BARBA E., QUIROGA S., ACCARINO A., MONCLÚS E., MALAGELADA C., BURRI E., NAVAZO I., MALAGELADA J., AZPIROZ F.: Mechanisms of abdominal distension in severe intestinal dysmotility: abdomino-thoracic response to gut retention. *Neurogastroenterology and motility* 25, 6 (2013), e389–e394. 1
- [BWK01] BARTROLÍ A. V., WEGENKITTL R., KÖNIG A., GRÖLLER M. E.: Nonlinear virtual colon unfolding. In *IEEE Visualization 2001, October 24–26, 2001, San Diego, CA, USA, Proceedings* (2001), pp. 411–420. 2
- [CVC*95] CLARKE L., VELTHUIZEN R., CAMACHO M., HEINE J., VAIDYANATHAN M., HALL L., THATCHER R., SILBINGER M.: MRI segmentation: Methods and applications. *Magnetic Resonance Imaging* 13, 3 (1995), 343–368. 1
- [HMG*16] HOAD C. L., MENYS A., Garsed K., MARCIANI L., HAMY V., MURRAY K., COSTIGAN C., ATKINSON D., MAJOR G., SPILLER R. C., TAYLOR S. A., GOWLAND P. A.: Colon wall motility: comparison of novel quantitative semi-automatic measurements using cine MRI. *Neurogastroenterology & Motility* 28, 3 (2016), 327–335. 2
- [JM13] JOHNSON H. J., MCCORMICK M., IBÁÑEZ L., CONSORTIUM T. I. S.: *The ITK Software Guide*, third ed. Kitware, Inc., 2013. In press. 4
- [JSNS17] JONGE C., SMOUT A., NEDERVEEN A., STOKER J.: Evaluation of gastrointestinal motility with MRI: Advances, challenges and opportunities. *Neurogastroenterology & Motility* 30, 1 (2017), e13257. 2
- [KSM*10] KLEIN S., STARING M., MURPHY K., VIERGEVER M. A., PLUIM J. P. W.: elastix: A toolbox for intensity-based medical image registration. *IEEE Transactions on Medical Imaging* 29, 1 (Jan 2010), 196–205. 8
- [LH97] LEWIS S. J., HEATON K. W.: Stool form scale as a useful guide to intestinal transit time. *Scandinavian Journal of Gastroenterology* 32, 9 (1997), 920–924. 6
- [LZ13] LU L., ZHAO J.: An improved method of automatic colon segmentation for virtual colon unfolding. *Computer Methods and Programs in Biomedicine* 109, 1 (2013), 1–12. 2
- [MBG*19] MARK E. B., BÄYDKER M. B., GRÄYNLUND D., ÅYSTERGAARD L. R., FRÄYKJÆR J. B., DREWES A. M.: MRI analysis of fecal volume and dryness: Validation study using an experimental oxycodone-induced constipation model. *Journal of Magnetic Resonance Imaging* (2019). 2, 8
- [MMPN*13] MONCLÚS E., MUÑOZ-PANDIELLA I., NAVAZO I., VÁZQUEZ P.-P., ACCARINO A., BARBA E., QUIROGA S., AZPIROZ F.: Morpho-volumetric measurement tools for abdominal distension diagnosis. In *XXIII Congreso Española de Informática Gráfica* (2013), pp. 39–48. 1, 2, 8, 9
- [NY08] NÄPPI J., YOSHIDA H.: Adaptive correction of the pseudo-enhancement of CT attenuation for fecal-tagging CT colonography. *Medical Image Analysis* 12, 4 (2008), 413–426. 2
- [OMB*18] ORELLANA B., MONCLÚS E., BRUNET P., NAVAZO I., BENDEZÚ A., AZPIROZ F.: Quasi-automatic colon segmentation on T2-MRI images with low user effort. In *Medical Image Computing and Computer Assisted Intervention - MICCAI 2018 - 21st International Conference, Granada, Spain, September 16–20, 2018, Proceedings, Part III* (2018), pp. 638–647. 9
- [PMB*18] POULSEN J. L., MARK E. B., BROCK C., FRÄYKJÆR J. B., KROGH K., M. D. A.: Colorectal transit and volume during treatment with prolonged-release oxycodone/naloxone versus oxycodone plus macrogol 3350. *Journal of Neurogastroenterology and Motility* 24 (2018), 119–127. 2
- [PMG*14] PRITCHARD S. E., MARCIANI L., Garsed K. C., HOAD C. L., THONGBORISUTE W., ROBERTS E., GOWLAND P. A., SPILLER R. C.: Fasting and postprandial volumes of the undisturbed colon: normal values and changes in diarrhea-predominant irritable bowel syndrome measured using serial MRI. *Neurogastroenterology & Motility* 26, 1 (2014), 124–130. 2
- [SNP*15] SANDBERG T. H., NILSSON M., POULSEN J. L., GRAM M., FRØKJÆR J. B., ØSTERGAARD L. R., DREWES A. M.: A novel semi-automatic segmentation method for volumetric assessment of the colon based on magnetic resonance imaging. *Abdominal Imaging* 40, 7 (2015), 2232–2241. 2, 4, 7, 8, 9
- [SZBN08] SUNDARAM P., ZOMORODIAN A., BEAULIEU C., NAPEL S.: Colon polyp detection using smoothed shape operators: Preliminary results. *Medical Image Analysis* 12, 2 (2008), 99–119. 2